Incomplete Multi-View Clustering Based on Joint Concept Decomposition and Anchor Graph Learning

Zhuowen Li, Hongmei Chen, Biao Xiang, Zhong Yuan, Chuan Luo and Tianrui Li

March 19, 2025

Incomplete multi-view clustering based on joint concept decomposition and anchor graph learning

Zhuowen Li[1,2,3,4], Hongmei Chen[✉1,2,3,4], Biao Xiang[1,2,3,4], Zhong Yuan[5], Chuan Luo[5], and Tianrui Li[1,2,3,4]

[1] School of Computing and Artificial Intelligence, Southwest Jiaotong University, Chengdu, 611756, China
[2] National Engineering Laboratory of Integrated Transportation Big Data Application Technology, Southwest Jiaotong University, Chengdu, 611756, China
[3] Engineering Research Center of Sustainable Urban Intelligent Transportation, Ministry of Education, Chengdu 611756, P.R. China
[4] Manufacturing Industry Chains Collaboration and Information Support Technology Key Laboratory of Sichuan Province, Southwest Jiaotong University, Chengdu 611756, P.R. China
[5] College of Computer Science, Sichuan University, Chengdu 610065, China
lizhuowen@my.swjtu.edu.cn; hmchen@swjtu.edu.cn; xiangbiao@my.swjtu.edu.cn; yuanzhong@scu.edu.cn; cluo@scu.edu.cn; trli@swjtu.edu.cn

Abstract. The main objective of incomplete multi-view clustering is to effectively utilize the existing view information to fill in the missing data and to mine the complementary information and potential associations between multiple views to effectively group samples. The existing primary means for recovering missing information are classified into two parts: one uses matrix decomposition or low-rank constraints to fill in the missing views, and the other constructs multiple graph structures and uses graph regularization to recover the corresponding missing parts. However, the two methods are relatively independent and are not used jointly to improve the model performance. This paper proposes an incomplete multi-view clustering method with complete clustering metrics and complete anchor graphs (CFAG). Specifically, each view's missing samples are recovered by a matrix of consistent clustering metrics and represented by an anchor graph. The recovered complete data performs anchor graph construction and anchor learning and utilizes the orthogonal variation principle to learn the consistency structure of multiple anchor graphs to mine the complementary information among multiple views. The clustering metrics are obtained based on the consistency structure, and the consistency of the clustering metrics is also considered to obtain the final clustering results. The effectiveness of the proposed method is verified on multiple datasets.

Keywords: Incomplete multi-view clustering · Missing views recovery · Anchor graph.

1 Introduction

In today's data-driven era, multi-view has become integral to many fields, such as computer vision, bioinformatics, and social network analysis [14]. Multi-view data consists of information collected from multiple perspectives or multiple sensors, and its inclusion provides a detailed and complementary description of the same set of objects [8]. For example, in image recognition, an image can contain multiple views, such as color, texture, and shape; in bioinformatics, a gene can have multiple views, such as its expression level, sequence information, and functional annotations. These views are independent and complementary, providing more comprehensive information for data analysis and pattern recognition [13]. This diversity of information provides more comprehensive data for machine learning models, especially in the task of clustering analysis [20]. Clustering analysis is an unsupervised learning method aiming to group similar objects. While traditional single-view clustering methods utilize data from only a single view for clustering, multi-view clustering attempts to integrate information from multiple views to improve the accuracy and robustness of clustering [15].

However, real-world data collection processes are often subject to constraints such as sensor failures, data transmission errors, or privacy safeguards, leading to the prevalence of missing views in multi-view data [9]. This incompleteness increases the complexity of data processing and poses a serious challenge to the performance of traditional multi-view clustering methods [25]. Therefore, effectively handling missing data to improve the performance of incomplete multi-view clustering has become a concern.

This year, a variety of methods have been proposed for incomplete multi-view data, which can be roughly classified into three categories: matrix-factorization-based methods, graph-based methods, and deep learning-based methods [12]. The matrix-factorization-based methods usually use matrix decomposition or self-representation to complete the missing data in multi-view and then perform clustering based on the complete data [16]. The core idea of this class of methods is to evaluate the missing data using the correlation between views [18]. In self-representation-based methods, a low-rank constraint guarantees that the multiple view matrices have consistent properties, where kernel-paradigm minimization is often utilized, which guarantees low rank by minimizing the kernel-paradigm of the matrix, i.e., the sum of singular values [19]. The graph-based approaches attempt to construct a consistent graph that utilizes complementarities between multiple views to reduce the impact of missing data and enable clustering on that graph [22]. The deep learning-based methods utilize the powerful representation capabilities of neural networks to learn a shared representation of multi-view data [3]. Such methods typically employ self-encoders or generative adversarial networks to learn low-dimensional representations of data. In addition, the subspace learning-based approaches perform clustering by finding the common subspace of the multi-view data [23].

Although the appeal methods deal with the problem of incompleteness to a certain extent, they still have some limitations. While these methods recover missing data, they do not take into account the consistency between the missing data. Graph-based methods are less efficient in dealing with high-dimensional data and simple graph fusion, thus failing to utilize complementary information. The consistency between multiple clustering indicator matrices is not considered when obtaining clustering labels. The paper proposes an incomplete multi-view clustering model based on conceptual decomposition (CFAG) to address the above issues, which utilizes cluster consistency to fill in missing data. Specifically, in missing data recovery, the clustering metrics of each view are combined with the original data matrix using conceptual decomposition, which adds a correlation matrix due to the different samples missing from each view. Based on this, anchor points and anchor graphs are used to explore further the data relationships between existing and missing data. Also, orthogonal variations are utilized to explore complementary and consistent information between multiple anchor graphs. The matrix decomposition is used to learn the clustering metrics for each view using the learnt consistency structure to align it with that in the conceptual decomposition. To integrate information from all views for global consistency, weighted spectral rotation is introduced to learn the final clustering results. The main contributions of this paper are as follows:

(i) The proposed method explores potential associations between incomplete data through conceptual decomposition and anchor graph learning, which recovers missing instances in incomplete data and complete data used for anchor learning.
(ii) To take advantage of the complementary information between multiple views, orthogonal changes are introduced to bridge the anchor graphs of the views. The clustering metrics for each view are not obtained in a single way but by both conceptual decomposition and consistent structural decomposition in order to explore the semantic associations between the views.
(iii) Spectral rotation is integrated into data recovery and consistency structure learning to obtain stable clustering results.

2 Related work

The following section focuses on two methods this paper uses: concept factorization and anchor graph learning.

2.1 Concept factorization

The principle of concept decomposition is to utilize multi-view consistency information to recover missing instances. Its main way is to utilize the correlation between different views to extract shared underlying concepts from multiple views. The core idea is that data from different views may reflect the same underlying structure, although they are represented differently. For example, Lu et al. used concept factorization to fuse helpful information and added two regularizations to force coefficient matrix smoothing and learn latent clustering structures [10]. Khan et al. dealt with the incomplete problem of views using weighted concept factorization, using common regularization constraints to obtain the shared structure, and introducing smoothed regularization to prevent overfitting [4]. Liu et al. used concept factorization in high-dimensional space to distinguish different classes of sample points and employed multiple graph regularization constraints to extract flow shape information from different views [6].

2.2 Anchor graph clustering

Anchor graph learning is used to reduce computational complexity, and the anchor points are usually representative sample points in the dataset to extract the intrinsic structure and underlying concepts of the data despite incomplete views. For example, Dai et al. projected the original space into the latent space and constructed multiple view-specific anchor graphs that were stacked into a graph tensor to capture higher-order correlations [2]. Li et al. learned inter-view anchor graphs and fused them into a consensus sparse anchor graph in which fast spectral clustering was applied to produce a single clustering result [5]. Zhang et al. adaptively learned discriminative anchors for each view, utilized matrix decomposition of the anchor graph matrix, and reached a consensus matrix prior to the k-mean algorithm [24].

3 Methodology

3.1 Preliminary

In the paper, uppercase font denotes matrices ($X \in R^{m\times n}$) and lowercase font denotes vectors ($x \in R^m$). For matrix X, X_{ij}, $X_{i:}$, and $X_{:j}$ denote the (i, j)th element of the matrix, the ith row vector, and the jth column vector, respectively. X^T, X^{-1}, and $Tr(X)$ denote the transpose, inverse, and trace of the matrix X, respectively. Meanwhile, $||X||_F = \sqrt{\sum_{i,j} X_{ij}^2}$ denotes the Frobenius norm of matrix X. For clarity, the mathematical symbols and explanations involved in the text are listed in Table 1.

3.2 Proposed method

Concept decomposition is introduced to explore the association between incomplete views and concepts, where concepts are identified as a matrix of clustering metrics for each view. Traditional conceptual decomposition decomposes the original data matrix into two matrices with potential dimensions c. The number of categories is substituted for c to avoid excessive discussion of c. This low-dimensional representation effectively reduces the dimensionality of the data and improves clustering performance. One of the matrices in the decomposition is represented by the existing data because at least one sample of the same medium category exists in this view to recover missing data, implying that the existing

Table 1: Commonly used notations.

Notations	Explanations
$X^v \in R^{d_v \times n_m}$	The incomplete multi-view data matrix of the vth view
$\tilde{X}^v \in R^{d_v \times n}$	The multi-view data matrix of the vth view after missing data filling
$W^v \in R^{n_m \times k}$	The association matrix of the vth view
$R^v \in R^{k \times n}$	The indicator matrix of the vth view
$B^v \in R^{d_v \times m}$	The anchor matrix of the vth view
$Z^v \in R^{m \times n}$	The anchor graph of the vth view
$A \in R^{m \times n}$	The essential anchor graph
$G^v \in R^{m \times m}$	The orthogonal graph of the vth view
$P \in R^{m \times k}$	The cross-view projection matrix
$F \in R^{n \times k}$	The clustering label matrix
$Q^v \in R^{k \times k}$	The rotation matrix of the vth view
d_v	The feature dimension of the vth view
n_m	The number of existing instances of the vth view
n	The number of instances
k	The number of clustering categories
m	The number of anchors

data can represent the missing data. For this purpose, the objective function is expressed as

$$min_{\tilde{X}^v, W^v, R^v} \sum_{v=1}^{l} ||\tilde{X}^v - X^v W^v R^v||_F^2 \quad s.t.\ W^v \geq 0, \tag{1}$$

where $\tilde{X}^v \in R^{d_v \times n}$ denotes the multi-view data matrix after recovering the missing data. $X^v \in R^{d_v \times n_m}$ denotes the incomplete multi-view data matrix. $W^v \in R^{n_m \times k}$ denotes the association matrix, which means the degree of correlation between the data matrices and the concepts. $W^v \geq 0$ implies that this correlation must be positive. $R^v \in R^{k \times n}$ denotes the indicator matrix.

The feature dimension d_v and the number of instances n of the original data matrix is much larger than the number of clustering categories k, resulting in a closely related computational cost for the process. A self-representation strategy is introduced to represent each data point using the original data to reduce this cost. However, there is a large amount of redundancy in the original space, so a small number of data points are selected to reconstruct the subspace. An anchor point strategy is used for this purpose, but now the anchor point strategy is divided into two parts: selection of anchor points and anchor graph learning, which are relatively independent. In order to combine these two processes, anchor points are learned using all samples, and the anchor graph is optimized at the same time. Based on this, the following objective function is constructed as

$$min_{\tilde{X}^v, B^v, Z^v} \sum_{v=1}^{l} ||\tilde{X}^v - B^v Z^v||_F^2 \quad s.t.\ {B^v}^T B^v = I, Z^v \geq 0, {Z^v}^T \mathbf{1} = \mathbf{1}, \tag{2}$$

where $B^v \in R^{d_v \times m}$ denotes the anchor matrix of the vth view and $Z^v \in R^(m \times n)$ denotes the anchor graph. In the experiment the number of anchor points is fixed as the number of clusters. The orthogonality constraint $B^{v^T} B^v = I$ ensures that the anchor points are independent of each other. The constraint on Z^v ensures that the relationship between each sample and anchor point is in a certain range. From Eq. (2), it is clear that the process not only learns anchor points and anchor graphs but also reconstructs the incomplete multi-view data matrix. To ensure that the missing data recovered by Eq. (2) and Eq. (1) are consistent while avoiding parametric effects, the following objective function is constructed as

$$
\begin{aligned}
& min_{W^v, R^v, B^v, Z^v} \sum_{v=1}^{l} ||X^v W^v R^v - B^v Z^v||_F^2 \\
& s.t.\ W^v \geq 0, B^{v^T} B^v = I, Z^v \geq 0, Z^{v^T} \mathbf{1} = \mathbf{1}.
\end{aligned} \tag{3}
$$

Eq. (3) recovers the missing data but does not utilize the complementary information of multiple views. The consistency structure is learned from the anchor graphs, but there are inconsistencies in the anchors across views. An orthogonal variation strategy is introduced to fuse multiple anchor graphs. The main element of this strategy is that for the matrix (X, Y) corresponding to the two dimensions, if Y is an orthogonal matrix, then $||X||_F^2 = ||YX||_F^2$. Based on this, assuming that X is the anchor graph for each view, a basic anchor graph can be learned using change of change with

$$
min_{A, G^v} ||A||_F^2 \quad s.t.\ \ G^{v^T} G^v = I, Z^v = G^v A, A \geq 0, A\mathbf{1} = \mathbf{1}, \tag{4}
$$

where $G^v \in R^{m \times m}$ corresponds to Y denoting the orthogonal matrix of the vth view. $A \in R^{m \times n}$ denotes the basic anchor graph. Complementary information between multiple views can be learned by varying the orthogonality of all anchor graphs.

When dealing with incomplete multi-view data, the missing instances differ between views, resulting in a suboptimal learned metrics matrix R^v at high missing rates. While exploring the intrinsic structure of multiple views, the global consistency of the intrinsic structure should also be considered, i.e., the indicator matrix R^v can be obtained from the underlying anchor graph. Therefore, cross-view consistency can be achieved by introducing the projection matrix, which takes advantage of the property that the multi-view data describes the same set of things, projecting R^v into the basic anchor graph. Thus getting rid of the inaccuracy of the indicator matrix R^v learned from Eq. (3). The objective function is expressed as

$$
min_{P, R^v} \sum_{v=1}^{l} ||A - PR^v||_F^2 \quad s.t.\ \ P^T P = I, R^v R^{v^T} = I, \tag{5}
$$

where $P \in R^{m \times k}$ denotes the cross-view projection matrix. The orthogonal constraint $R^v R^{v^T} = I$ ensures that the indicators are independent. Eq. (5) not only ensures the accuracy of the learned metrics matrix but also restricts each other with anchor graph learning, making the recovery data reliable and mitigating the negative impact of view-specific missing data.

The indicator matrices of the complete views do not take into account the differences between the views and, therefore, cannot be used for the final clustering, but they have the same clustering structure. Therefore, spectral rotation is introduced to obtain the final clustering results, and its main objective is to minimize the distance between $R^{v^T}Q^v$ and the final clustering label matrix, where Q^v is an orthogonal rotation matrix. The objective function is expressed as

$$min_{F,R^v,Q^v} \sum_{v=1}^{l} ||F - R^{v^T}Q^v||_F^2 \quad s.t. \;\; Q^{vT}Q^v = I, F \in Ind, \tag{6}$$

$F \in Ind$ ensures that the clustering labelling matrix $F \in R^{n \times k}$ has only one element of 1 in each row, and the rest are 0.

Combining concept decomposition, anchor graph learning, and clustering structure learning will help explore the underlying connections between data in incomplete multi-view to reduce the impact of missing instances. In addition, orthogonal transformations and spectral rotations are used to make the indicator matrices consistent across learning processes to obtain stable clustering results. Considering the different contributions of each view, adaptive weights are introduced to measure them. The overall objective function is obtained by combining Eqs. (3), (4), (5), and (6) as

$$\begin{aligned}
&min_{\Psi} \sum_{v=1}^{l} ||X^vW^vR^v - B^vZ^v||_F^2 + \lambda_1||A||_F^2 + \sum_{v=1}^{l} \Big(\lambda_2\alpha^{v^2}||A - PR^v||_F^2 \\
&+ \lambda_3\beta^{v^2}||F - R^{v^T}Q^v||_F^2\Big) \; s.t. \; W^v \geq 0, B^{v^T}B^v = I, R^vR^{v^T} = I, Z^v \geq 0, \\
&Z^{v^T}\mathbf{1} = \mathbf{1}, G^{v^T}G^v = I, Z^v = G^vA, A \geq 0, A\mathbf{1} = \mathbf{1}, P^TP = I, Q^{vT}Q^v = I, \\
&F \in Ind, \sum_{v=1}^{l}\alpha^v = 1, \alpha^v \geq 0, \sum_{v=1}^{l}\beta^v = 1, \beta^v \geq 0.
\end{aligned} \tag{7}$$

where $\Psi = \{W^v, R^v, B^v, Z^v, A, G^v, P, F, Q^v, \alpha^v, \beta^v\}$ denotes the variables to be optimized. λ_1, λ_2, and λ_3 are balance parameters.

3.3 Optimization

Eq. (7) is solved using alternating iterations and introducing the intermediate variable Y^v to solve the equation constraint $Z^v = G^vA$. Eq. (7) is transformed using the Lagrange multiplier method.

$$\begin{aligned}
\mathcal{L}_{\Omega} = &\sum_{v=1}^{l} ||X^vW^vR^v - B^vZ^v||_F^2 + \lambda_1||A||_F^2 + \sum_{v=1}^{l} \Big(\lambda_2\alpha^{v^2}||A - PR^v||_F^2 \\
&+ \lambda_3\beta^{v^2}||F - R^{v^T}Q^v||_F^2 + \frac{\rho}{2}||Z^v - G^vA + \frac{Y^v}{\rho}||_F^2\Big)
\end{aligned} \tag{8}$$

In Eq. (8), $\Omega = \{W^v, R^v, B^v, Z^v, A, G^v, P, F, Q^v, \alpha^v, \beta^v\}$, Y^v is the Lagrange multiplier, and ρ is the penalty factor. Transform Eq. (8) into the following stepwise optimization problem:

B^v*-subproblem* : When the remaining variables are fixed, the optimization problem for B^v transforms into

$$min_{B^v} \sum_{v=1}^{l} ||X^v W^v R^v - B^v Z^v||_F^2 \quad s.t. \;\; B^{v^T} B^v = I. \tag{9}$$

Since B^v is independent of each other between views, Eq. (9) transforms to

$$max_{B^v} Tr(B^{v^T} M^v) \quad s.t. \;\; B^{v^T} B^v = I, \tag{10}$$

where $M^v = X^v W^v R^v Z^{v^T}$. By performing an SVD decomposition of M^v, the optimal solution of B^v is UV^T, and U and V are the left and right singular value matrices of M^v, respectively.

Z^v*-subproblem* : When the remaining variables are fixed, the optimization problem for Z^v of each view transforms into

$$min_{Z^v} ||X^v W^v R^v - B^v Z^v||_F^2 + \frac{\rho}{2} ||Z^v - G^v A + \frac{Y^v}{\rho}||_F^2. \tag{11}$$

Optimizing each column $Z^v_{:j}$ of Z^v alone, Eq. (11) transforms to

$$min_{Z^v_{:j}} \frac{1}{2} Z^{v^T}_{:j} C^v_Z Z^v_{:j} + f_Z Z^v_{:j} \quad s.t. \;\; Z^v_{:j} \geq 0, Z^{v^T}_{:j} \mathbf{1} = 1, \tag{12}$$

where $C^v_Z = 2B^{v^T} B^v + \rho I$, $f_Z = Y^{v^T}_{:j} - 2(X^v W^v R^v)^T_{:j} B^v - 2A^T_{:j} G^{v^T}$. Eq. (12) is a quadratic programming problem.

W^v*-subproblem* : When the remaining variables are fixed, the optimization problem for W^v of each view transforms into

$$min_{W^v} ||X^v W^v R^v - B^v Z^v||_F^2 \quad s.t. \;\; W^v \geq 0. \tag{13}$$

Find the derivative of Eq. (13) with respect to W^v and let the derivative be 0 and the optimal solution to W^v that can be obtained using the KKT condition as

$$W^v_{ij} = \left(\frac{(X^{v^T} B^v Z^v R^{v^T})_{ij}}{(X^{v^T} X^v W^v R^v R^{v^T})_{ij}} \right)^{\frac{1}{2}} W^v_{ij}. \tag{14}$$

R^v-subproblem : When the remaining variables are fixed, the optimization problem for R^v of each view transforms into

$$min_{R^v}||X^vW^vR^v-B^vZ^v||_F^2+\lambda_2\alpha^{v^2}||A-PR^v||_F^2+\lambda_3\beta^{v^2}||F-R^{v^T}Q^v||_F^2. \quad (15)$$

Its optimization problem is similar to B^v, the optimal solution of R^v is UV^T, and U, V are the left and right singular value matrices of $W^{v^T}X^vB^vZ^v-\lambda_2\alpha^{v^2}P^TA-\lambda_3\beta^{v^2}Q^vF^T$ respectively.

A-subproblem : When the remaining variables are fixed, the optimization problem for A transforms into

$$\begin{aligned}&min_A\lambda_1||A||_F^2+\sum_{v=1}^{l}\Big(\lambda_2\alpha^{v^2}||A-PR^v||_F^2+\frac{\rho}{2}||Z^v-G^vA+\frac{Y^v}{\rho}||_F^2\Big)\\&s.t. A\geq 0, A\mathbf{1}=\mathbf{1}.\end{aligned} \quad (16)$$

This optimization is similar to Z^v, and optimizing $A_{:j}$ alone yields

$$min_A\frac{1}{2}A_{:j}^TC_A^vA_{:j}+f_AA_{:j} \quad s.t.\ \ A_{:j}\geq 0, A_{:j}^T\mathbf{1}=1, \quad (17)$$

where $C_A^v=(2\lambda_1+2\lambda_2\sum_{v=1}^{l}\alpha^{v^2}+\rho l)I,\ f_A=\sum_{v=1}^{l}(Y_{;j}^{v^T}G^v-2\lambda_2R_{;j}^{v^T}P^T-\rho Z_{;j}^{v^T}G^v)$. The optimal solution of A can be obtained using the quadratic programming function.

G^v-subproblem : When the remaining variables are fixed, the optimization problem for G^v transforms into

$$min_{G}v||Z^v-G^vA+\frac{Y^v}{\rho}||_F^2 \quad s.t.\ \ G^{v^T}G^v=I. \quad (18)$$

Similar to B^v, the optimal solution of G^v is UV^T, and U, V are the left and right singular value matrices of $(Z^v-\frac{Y^v}{\rho})A^T$, respectively.

P-subproblem : When the remaining variables are fixed, the optimization problem for P transforms into

$$min_P\sum_{v=1}^{l}\alpha^{v^2}||A-PR^v||_F^2 \quad s.t.\ \ P^TP=I. \quad (19)$$

Similar to B^v, the optimal solution of P is UV^T, and U, V are the left and right singular value matrices of $\sum_{v=1}^{l}\alpha^{v^2}AR^{v^T}$, respectively.

Q^v-subproblem : When the remaining variables are fixed, the optimization problem for Q^v transforms into

$$min_{Q^v} {\beta^v}^2 ||F - {R^v}^T Q^v||_F^2 \quad s.t. \;\; {Q^v}^T Q^v = I. \tag{20}$$

Similar to B^v, the optimal solution of Q^v is UV^T, and U, V are the left and right singular value matrices of ${\beta^v}^2 R^v F$, respectively.

F-subproblem : When the remaining variables are fixed, the optimization problem for F transforms into

$$min_F \sum_{v=1}^{l} \lambda_3 {\beta^v}^2 ||F - {R^v}^T Q^v||_F^2 \quad s.t. \;\; F \in Ind. \tag{21}$$

Transform Eq. (21) into a trace as

$$max_F Tr(F^T O) \quad s.t. \;\; F \in Ind, \tag{22}$$

where $O = \lambda_3 \sum_{v=1}^{l} {\beta^v}^2 {R^v}^T Q^v$, then the optimal solution of F is

$$F_{ij} = \begin{cases} 1, if \;\; j = argmax_j O_{ij} \\ 0, otherwise. \end{cases} \tag{23}$$

α^v, β^v-subproblem : When the remaining variables are fixed, the optimization problem for α^v transforms into

$$min_\alpha \sum_{v=1}^{l} {\alpha^v}^2 q^v \quad s.t. \;\; \alpha \geq 0, \alpha \mathbf{1} = 1, \tag{24}$$

where $q^v = ||A - PR^v||_F^2$, $\alpha = [\alpha^1, \alpha^2, \ldots, \alpha^l]^T$. Eq. (24) is derived for α^v and the optimal solution for α^v according to the KKT condition as

$$\alpha^v = \frac{1}{q^v} (\sum_{v=1}^{l} \frac{1}{q^v})^{-1}. \tag{25}$$

The optimization of β^v is similar to α^v. Its optimal solution is $\frac{1}{p^v}(\sum_{v=1}^{l} \frac{1}{p^v})^{-1}$, where $p^v = ||F - {R^v}^T Q^v||_F^2$.

Y^v, ρ-subproblem : These two variables are updated as

$$Y^v = Y^v + \rho(Z^v - G^v A) \tag{26}$$
$$\rho = min\,(pho * \rho, \mu)\,. \tag{27}$$

where pho, μ are constants.

The computational complexity of each solution process is calculated to determine the total computational complexity of the proposed method. The total computational complexity of the proposed method is $O(k^2 d_v + lmk^3 + lnk^3 + n_m k^2 + nk^2)$.

4 Experiments

4.1 Datasets

The experiment consists of five datasets, namely 3Sources, 100leaves, Caltech101, and HW, whose details are shown in Table 2. Making p instances of each view in the above dataset missing at random (missing rate is p/n) to construct an incomplete multi-view dataset.

Table 2: Details of the datasets.

Dataset	3Sources	100leaves	Caltech101	HW
# Size	169	1600	1474	2000
# Classes	6	100	7	10
# View1	3560	64	48	240
# View2	3631	64	40	76
# View3	3068	64	254	216
# View4	-	-	198	47
# View5	-	-	512	64
# View3	-	-	928	6

4.2 Comparison methods

The following methods are compared to verify the validity of CFAG.

(i) HCLS_CGL [17]: It constructs a confidence graph on the raw data to learn a consistent representation and obtains the clustering structure through a consensus graph across views.

(ii) ETLSRR [21]: It constructs in-view similarity maps, stacks them into third-order tensors, and uses tensor decomposition to decompose it into sparse tensors and intrinsic tensors to model noise and underlying real data similarity, respectively.

(iii) JPLTD [11]: It utilizes orthogonal projection matrices to project the original data into a low-dimensional space, constructs view-specific similarity graphs, and stacks them into a third-order low-rank tensor, which is robustly clustered using a graph filter based on tensor decomposition.

(iv) FIMVC-VIA [7]: It learns view-independent anchor matrices to explore complementarities while constructing consensus anchor graphs based on a consistent clustering structure.

(v) CGCTD [1]: It utilizes confidence graphs to construct complete graphs, stacks them into tensors, and introduces the underlying tensor to recover accurate affine graphs.

4.3 Clustering results and analysis

Table 3 presents the evaluation metrics (ACC, NMI, and Purity) of the proposed method and the comparison algorithm when the missing rate is 0.1, and the bold font in the table indicates the best. The table shows that the proposed method (CFAG) performs better than the comparison algorithm on all datasets. This phenomenon indicates that the strategy adopted by the proposed method is effective in dealing with incomplete data and can fully exploit the complementarity and consistency between views.

Table 3: Algorithms' performance with a missing rate of 0.1.

Datasets	HCLS_CGL	ETLSRR	JPLTD	FIMVC-VIA	CGCTD	CFAG
ACC						
3Sources	70.93±0.72	74.20±1.95	73.70±16.21	69.22±0.76	72.71±2.51	**79.51±0.89**
100leaves	67.76±0.81	56.44±1.94	60.52±0.20	63.06±1.26	65.62±0.50	**70.35±0.42**
Caltech101	67.72±2.62	67.01±8.30	74.74±21.14	74.68±5.96	71.12±6.74	**76.11±4.12**
HW	83.04±3.99	85.00±0.20	77.64±15.55	85.00±6.00	75.25±0.34	**88.76±2.19**
NMI						
3Sources	70.93±0.33	72.78±8.75	74.54±16.11	69.22±0.23	74.12±2.94	**78.89±0.95**
100leaves	68.58±0.80	57.56±2.15	61.57±0.19	62.58±1.25	65.89±0.48	**71.00±5.69**
Caltech101	66.88±2.70	64.72±0.76	76.02±22.03	75.67±5.98	78.81±5.96	**81.18±1.18**
HW	80.38±8.65	84.04±1.20	75.73±15.83	80.09±1.38	73.41±0.49	**85.07±8.29**
Purity						
3Sources	71.43±0.28	69.64±4.20	72.61±16.48	60.49±0.16	73.52±2.39	**77.09±0.69**
100leaves	68.71±0.77	57.19±1.50	61.82±0.17	64.85±1.11	65.23±0.57	**69.35±1.72**
Caltech101	67.74±2.70	64.93±0.46	66.91±21.66	76.57±5.98	73.16±6.43	**78.18±8.18**
HW	83.04±9.09	80.49±3.60	79.37±16.29	84.96±2.40	74.78±0.12	**88.07±2.85**

Considering the effect of the missing rate on all the algorithms, experiments with different missing rates are conducted, and the experimental results are shown in Fig. 1. It can be seen that the performance of all algorithms decreases when the missing rate increases. However, on the 3Sources dataset, the decreasing trend of the performance of the proposed method (CFAG) is obvious when the missing rate changes from 0.5 to 0.7. In general, the metrics curves of ACC, NMI, and Purity of the proposed method (CFAG) are at the upper level, which also indicates the superiority of the performance of CFAG.

4.4 Sensitivity analysis

The proposed method involves three parameters which are λ_1 to control the basic anchor graph learning ($||A||_F^2$), λ_2 to control the complete indicator learning ($||A-PR^v||_F^2$) and λ_3 to control the clustering matrix learning ($||F-R^{v^T}Q^v||_F^2$). By fixing one parameter to change the others, the model's performance on the dataset is used to determine the optimal parameter combination. The variation of CAFG with different parameter combinations on 3Sources is shown in Fig. 2. From this, it can be seen that CAFG performs better when λ_1 and λ_3 take larger values.

4.5 Convergence analysis

This experiment verifies that the proposed optimization method is convergent, and the variation curve of the objective function is shown in Fig. 3. From this, it can be seen that the value of the objective function converges when the iteration is up to 20 times.

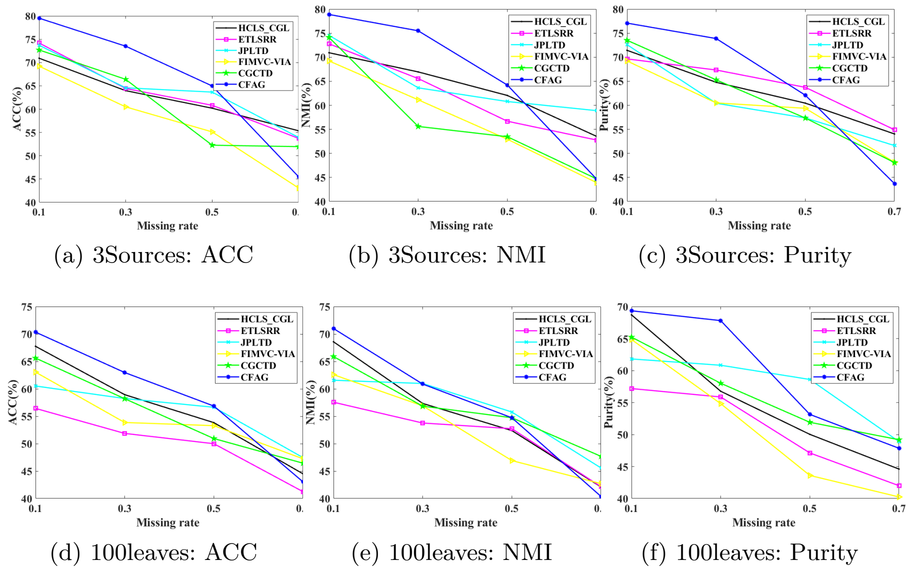

(a) 3Sources: ACC (b) 3Sources: NMI (c) 3Sources: Purity

(d) 100leaves: ACC (e) 100leaves: NMI (f) 100leaves: Purity

Fig. 1: ACC VS. missing rate on the 3Sources and 100leaves.

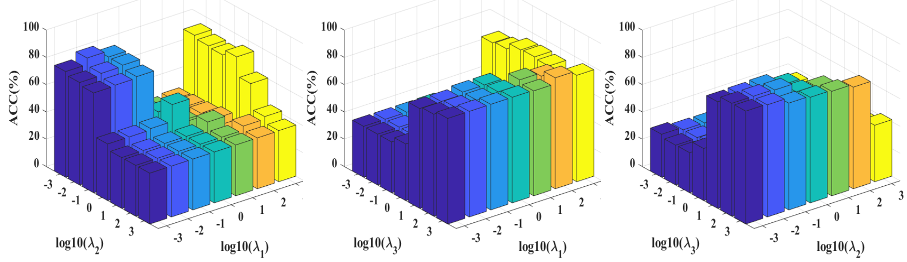

(a) 3Sources: λ_1, λ_2 (b) 3Sources: λ_1, λ_2 (c) 3Sources: λ_2, λ_3

Fig. 2: Variation of ACC of CFAG on 3Sources with different parameters.

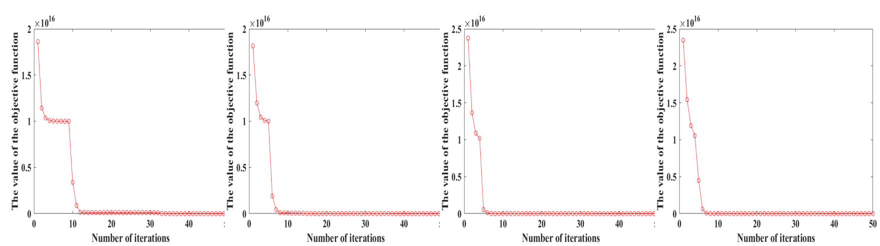

(a) 3Sources (b) 100leaves (c) Caltech101 (d) HW

Fig. 3: Variation of the objective function value with iterations.

5 Conclusions

This paper proposes a unified framework for recovering missing instances by joint concept decomposition and anchor graph learning. The proposed method exploits the consistency between views through conceptual decomposition and combines anchor graph learning to reduce the impact of missing data in the original space. Based on this, orthogonal variations are utilized to exploit the complements between views while combining with spectral rotation to achieve one-step clustering. Although the experiments show the effectiveness of the proposed method, there are some limitations. The number of anchor points in anchor graph learning is difficult to determine. The model contains multiple variables, which may lead to a local optimization when optimizing.

Acknowledgments. This work was supported by the National Natural Science Foundation of China (Nos. 62376230, 62076171, and 62306196).

References

1. Cheng, Y., Song, P.: Incomplete multi-view clustering via confidence graph completion based tensor decomposition. Expert Systems with Applications **258**, 125151 (2024)
2. Dai, J., Ren, Z., Luo, Y., Song, H., Yang, J.: Tensorized anchor graph learning for large-scale multi-view clustering. Cognitive Computation **15**(5), 1581–1592 (Sep 2023)
3. Huang, H., Yan, X., Zheng, Y., He, J., Xu, L., Qin, D.: Multi-view stereo algorithms based on deep learning: a survey. Multimedia Tools and Applications **84**(6), 2877–2908 (Feb 2025)
4. Khan, G.A., Khan, J., Anwar, T., Al-Huda, Z., Diallo, B., Ahmad, N.: Complementary incomplete weighted concept factorization methods for multi-view clustering. Knowledge and Information Systems **66**(12), 7469–7494 (Dec 2024)
5. Li, A., Feng, C., Wang, Z., Sun, Y., Wang, Z., Sun, L.: Anchor-based sparse subspace incomplete multi-view clustering. Wireless Networks **30**(6), 5559–5570 (Aug 2024)
6. Liu, G., Ge, H., Li, T., Su, S., Gao, P.: Robust multi-view clustering via collaborative constraints and multi-layer concept factorization. Applied Intelligence **54**(19), 9446–9463 (Oct 2024)
7. Liu, S., Liu, X., Wang, S., Niu, X., Zhu, E.: Fast incomplete multi-view clustering with view-independent anchors. IEEE Transactions on Neural Networks and Learning Systems **35**(6), 7740–7751 (2024)
8. Liu, Y., Zhu, C.: Dmvmlc-vt: Deep incomplete multi-view multi-label image classification with view translation and pseudo-label enhancement. The Visual Computer (Nov 2024)
9. Liu, Y., Zhu, C.: Dmvmlc-vt: Deep incomplete multi-view multi-label image classification with view translation and pseudo-label enhancement. The Visual Computer (Nov 2024)
10. Lu, M., Zhang, L., Li, F.: Adaptively local consistent concept factorization for multi-view clustering. Soft Computing **26**(3), 1043–1055 (Feb 2022)

11. Lv, W., Zhang, C., Li, H., Jia, X., Chen, C.: Joint projection learning and tensor decomposition-based incomplete multiview clustering. IEEE Transactions on Neural Networks and Learning Systems **35**(12), 17559–17570 (2024)
12. Niu, X., Zhao, X., Hu, L., Zhang, J.: An incomplete multi-view clustering approach using subspace alignment constraint. International Journal of Machine Learning and Cybernetics (Oct 2024)
13. Shi, W., Yin, A., Li, Y., Qian, B.: Cross-view transformer for enhanced multi-view 3d reconstruction. The Visual Computer (Nov 2024)
14. Singh, R., Kumar, V.: Ensemble multi-view feature set partitioning method for effective multi-view learning. Knowledge and Information Systems **66**(8), 4957–5001 (Aug 2024)
15. Tian, L., Peng, S.J., Liu, X., Chen, Y., Cao, J.: Multi-view anomaly detection via hybrid instance-neighborhood aligning and cross-view reasoning. Multimedia Systems **30**(6), 314 (Oct 2024)
16. Wang, Y., Yang, Y., Ning, T.: Local structure learning for incomplete multi-view clustering. Applied Intelligence **54**(4), 3308–3324 (Feb 2024)
17. Wen, J., Liu, C., Xu, G., Wu, Z., Huang, C., Fei, L., Xu, Y.: Highly confident local structure based consensus graph learning for incomplete multi-view clustering. In: 2023 IEEE/CVF Conference on Computer Vision and Pattern Recognition (CVPR). pp. 15712–15721 (2023)
18. Xue, S., Zhu, C.: Sadcl-net: Sparse-driven attention with dual-consistency learning network for incomplete multi-view clustering. Multimedia Systems **30**(5), 280 (Sep 2024)
19. Yin, J., Jiang, J.: Incomplete multi-view clustering based on self-representation. Neural Processing Letters **55**(7), 8673–8687 (Dec 2023)
20. Yu, Z., Dong, Z., Yu, C., Yang, K., Fan, Z., Chen, C.L.P.: A review on multi-view learning. Frontiers of Computer Science **19**(7), 197334 (Dec 2024)
21. Zhang, C., Li, H., Lv, W., Huang, Z., Gao, Y., Chen, C.: Enhanced tensor low-rank and sparse representation recovery for incomplete multi-view clustering. In: Thirty-Seventh AAAI Conference on Artificial Intelligence. pp. 11174–11182 (2023)
22. Zhang, K., Liu, B., Du, S., Yu, Y., Song, J.: Incomplete multi-view clustering based on low-rank representation with adaptive graph regularization. Soft Computing **27**(11), 7131–7146 (Jun 2023)
23. Zhang, Y., Zhu, C.: Incomplete multi-view clustering via attention-based contrast learning. International Journal of Machine Learning and Cybernetics **14**(12), 4101–4117 (Dec 2023)
24. Zhang, Z., Huang, Y.: Flexible anchor-based multi-view clustering with low-rank decomposition. International Journal of Machine Learning and Cybernetics (Nov 2024)
25. Zhu, C., Han, L.: A multi-view multi-label learning with incomplete data and self-adaptive correlations. International Journal of Machine Learning and Cybernetics (Jan 2025)